Supporting information

for

Non-Symmetrically Fused Bis(arylimino)pyridines with *Para-Phenyl Substitution: Exploring Their Use as *N',N,N''*-Supports in Iron Ethylene Polymerization Catalysis

Yizhou Wang [1,2], **Zheng Wang** [1,3], **Qiuyue Zhang** [1], **Yanping Ma** [1], **Gregory A. Solan** [1,4,*], **Yang Sun** [1] **and Wen-Hua Sun** [1,2,*]

[1] Key Laboratory of Engineering Plastics and Beijing National Laboratory for Molecular Sciences, Institute of Chemistry Chinese Academy of Sciences, Beijing 100190, China; wangyizhou13@iccas.ac.cn (Y.W.); wangzheng@iccas.ac.cn (Z.W.); zhangqiuyue@iccas.ac.cn (Q.Z.); myanping@iccas.ac.cn (Y.M.); sy0471103@iccas.ac.cn (Y.S.)

[2] CAS Research/Education Center for Excellence in Molecular Sciences, University of Chinese Academy of Sciences, Beijing 100049, China

[3] College of Science, Hebei Agricultural University, Baoding 071001, China
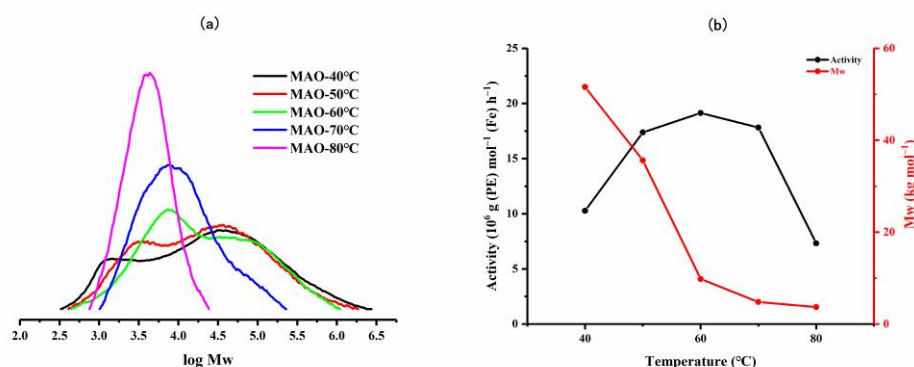
[4] Department of Chemistry, University of Leicester, University Road, Leicester LE1 7RH, UK

[*] Correspondence: gas8@leicester.ac.uk (G.A.S.); whsun@iccas.ac.cn (W.-H.S.); Tel.: +44-(0)116-2522096 (G.A.S.); +86-10-6255-7955 (W.-H.S.)
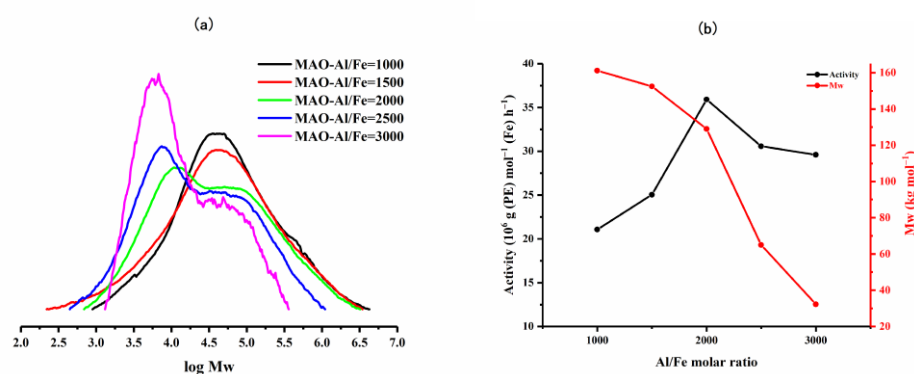
Table of Contents

1. GPC traces of selected polyethylenes along with plots of activity and polymer molecular weight as a function of various parameters
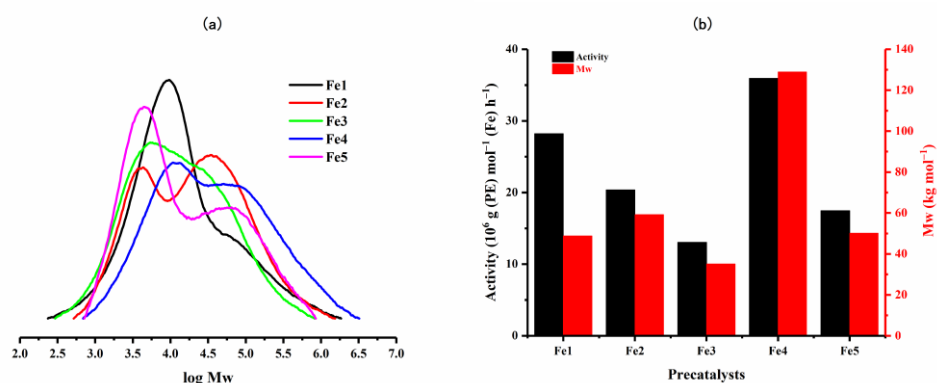

Figure S1. (**a**) GPC traces for the polyethylenes generated using **Fe4**/MAO at different run temperatures and (**b**) plots of catalytic activity and polymer molecular weight as function of run temperature.

Figure S2. (**a**) GPC traces for the polyethylenes generated using **Fe4**/MAO at various Al:Fe molar ratios and (**b**) plots of catalytic activity and polymer molecular weight as a function of Al:Fe molar ratio.
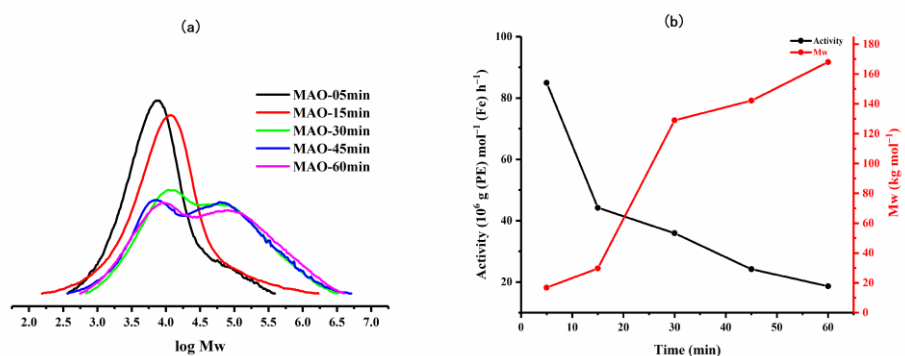

Figure S3. (**a**) GPC traces for the polyethylenes generated using **Fe4**/MAO over reaction time and (**b**) plots of catalytic activity and polymer molecular weight as a function of reaction time.

Figure S4. (**a**) GPC traces for the polyethylenes generated using **Fe1–Fe5** under MAO activation and (**b**) a bar chart showing the effects of variation in *N*-aryl group in **Fe1–Fe5** on catalytic activity and polymer molecular weight.
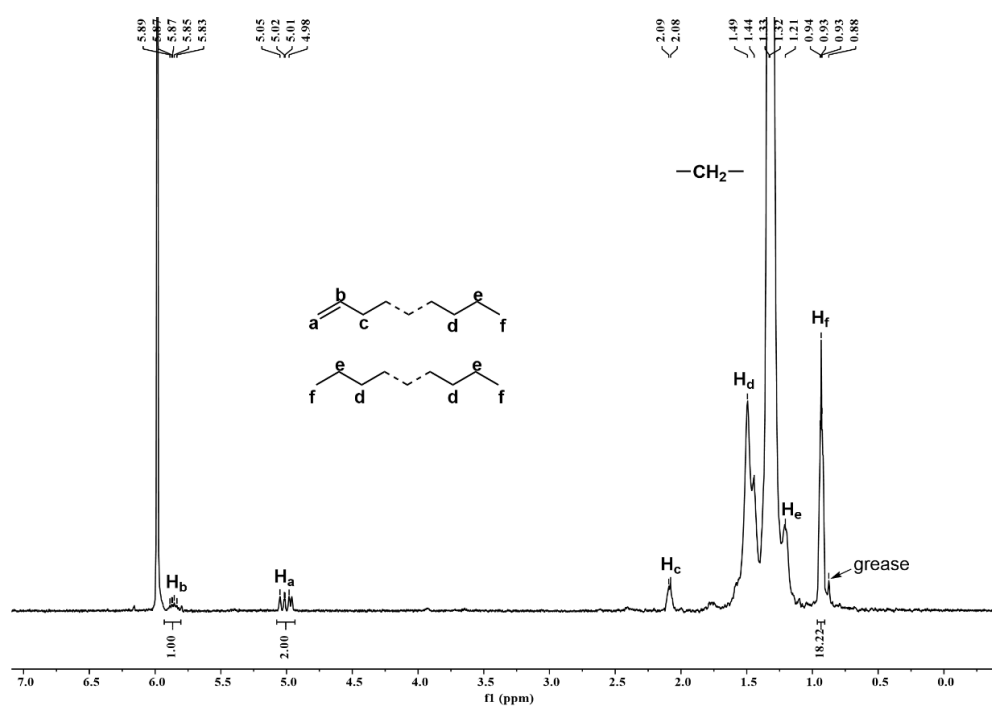
2.1. ^{1}H NMR spectra of selected polyethylenes
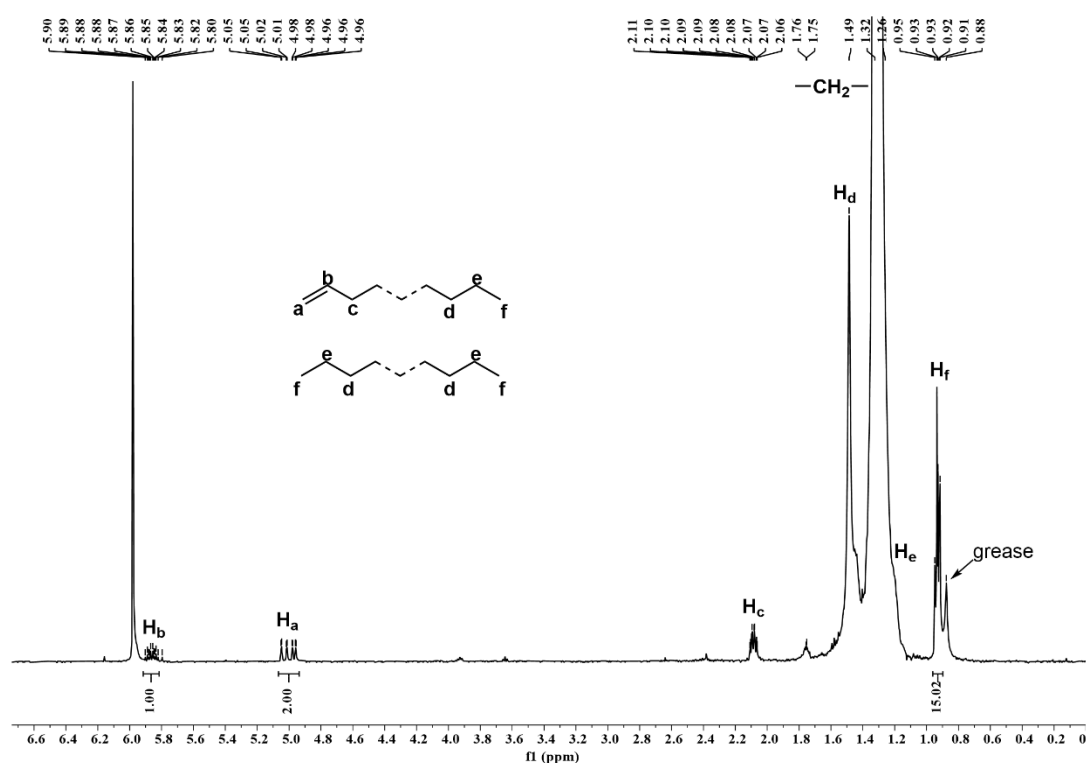
Figure S5. ^{1}H NMR spectrum of the polyethylene produced using **Fe4**/MMAO operating at 70 °C (entry 4, Table 2); recorded at 100 °C in 1,1,2,2-tetrachloroethane-*d*$_2$. The weak signal at *ca.* 0.87–0.88 ppm is attributed to the protons belonging to the methyl group in grease [1].
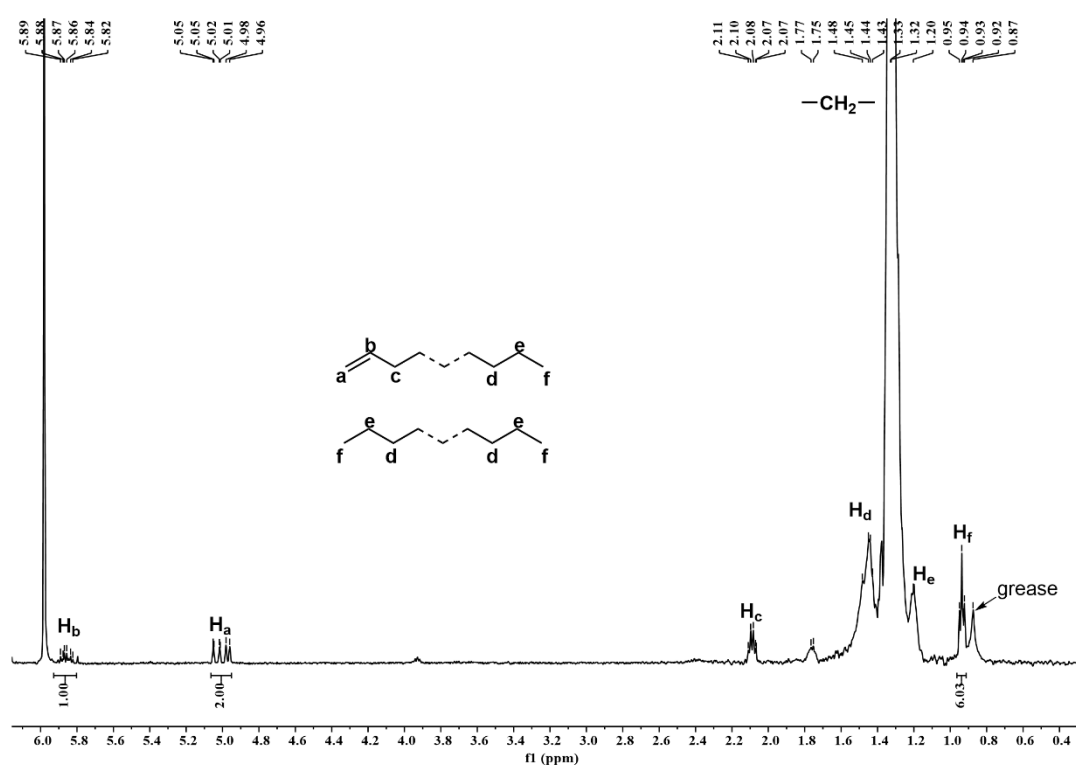
Figure S6. ^{1}H NMR spectrum of the polyethylene produced using **Fe4**/MMAO operating at 60 °C (entry 3, Table 2); recorded at 100 °C in 1,1,2,2-tetrachloroethane-*d*₂. The weak signal at *ca.* 0.87–0.88 ppm is attributed to the protons belonging to the methyl group in grease [1].

Figure S7. ^{1}H NMR spectrum of the polyethylene produced using **Fe4**/MMAO operating at 50 °C (entry 2, Table 2); recorded at 100 °C in 1,1,2,2-tetrachloroethane-*d*₂. The weak signal at *ca.* 0.87–0.88 ppm is attributed to the protons belonging to the methyl group in grease [1].
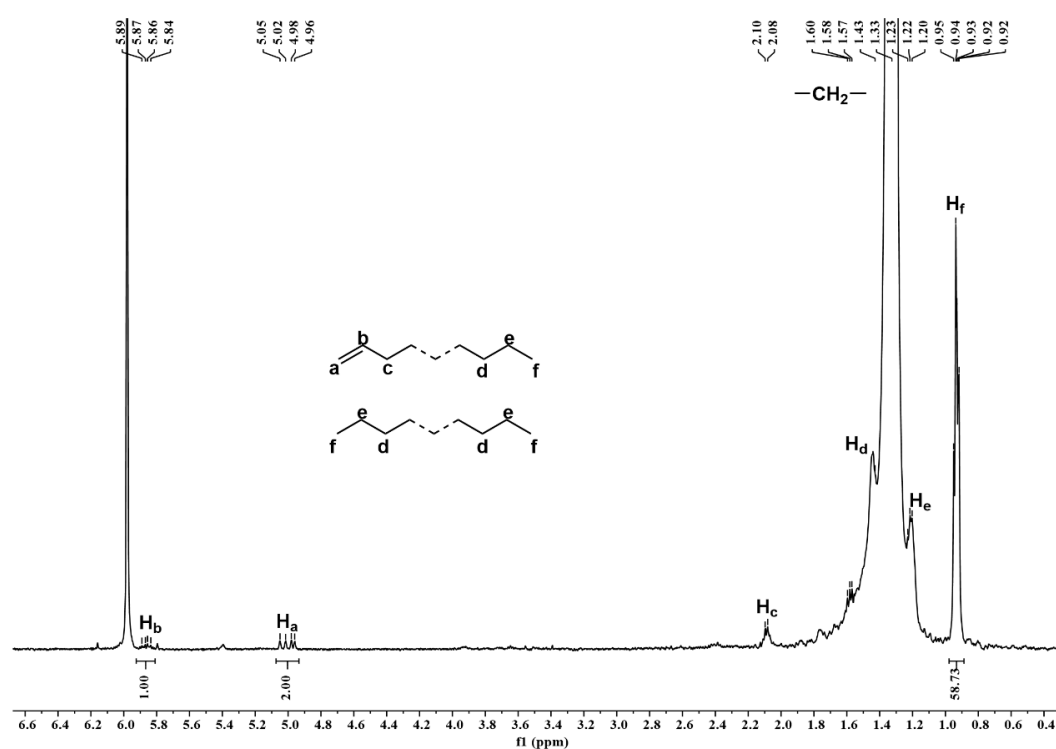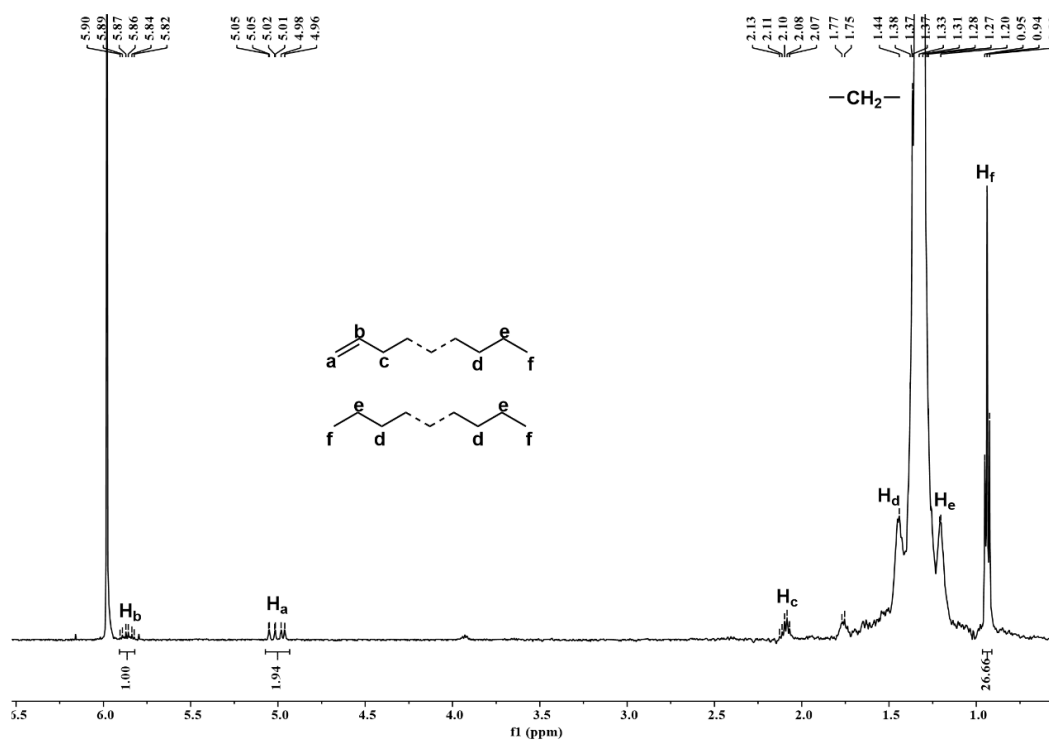
Figure S8. ^{1}H NMR spectrum of the polyethylene produced using **Fe4**/MMAO operating at 40 °C (entry 1, Table 2); recorded at 100 °C in 1,1,2,2-tetrachloroethane-d_2.

Figure S9. ^{1}H NMR spectrum of the polyethylene produced using **Fe4**/MAO operating at 40 °C (entry 1, Table 3); recorded at 100 °C in 1,1,2,2-tetrachloroethane-d_2.

Figure S10. ^{1}H NMR spectrum of the polyethylene produced using **Fe4**/MAO operating at 50 °C (entry 2, Table 3); recorded at 100 °C in 1,1,2,2-tetrachloroethane-d_2.

Figure S11. ^{1}H NMR spectrum of the polyethylene produced using **Fe4**/MAO operating at 60 °C (entry 3, Table 3); recorded at 100 °C in 1,1,2,2-tetrachloroethane-d_2.

Figure S12. ^{1}H NMR spectrum of the polyethylene produced using **Fe4**/MAO operating at 70 °C (entry 4, Table 3); recorded at 100 °C in 1,1,2,2-tetrachloroethane-d_2. The weak signal at *ca.* 0.87–0.88 ppm is attributed to the protons belonging to the methyl group in grease [1].
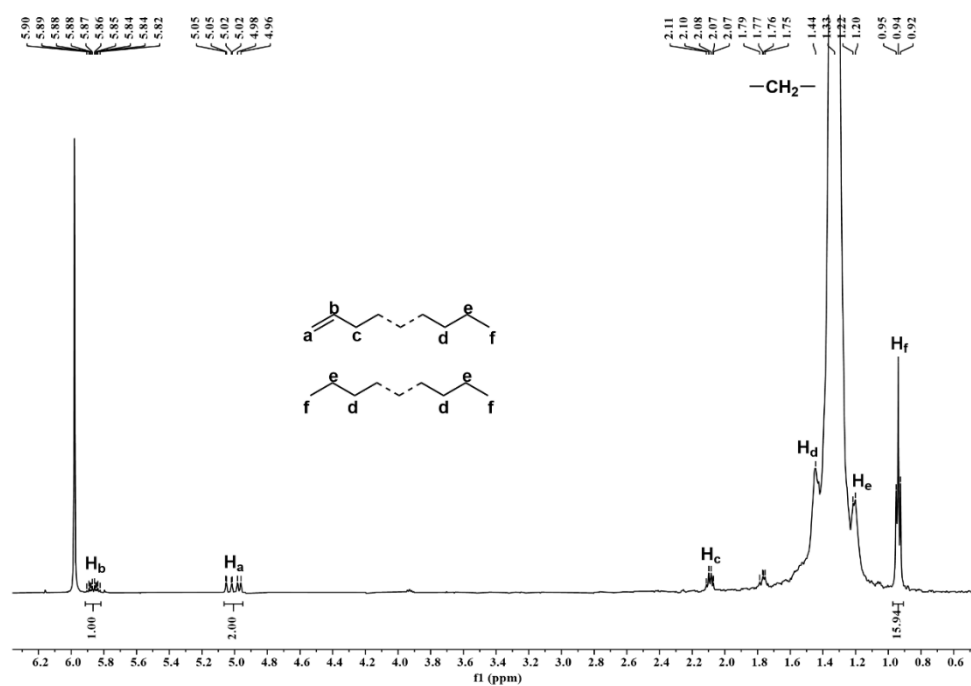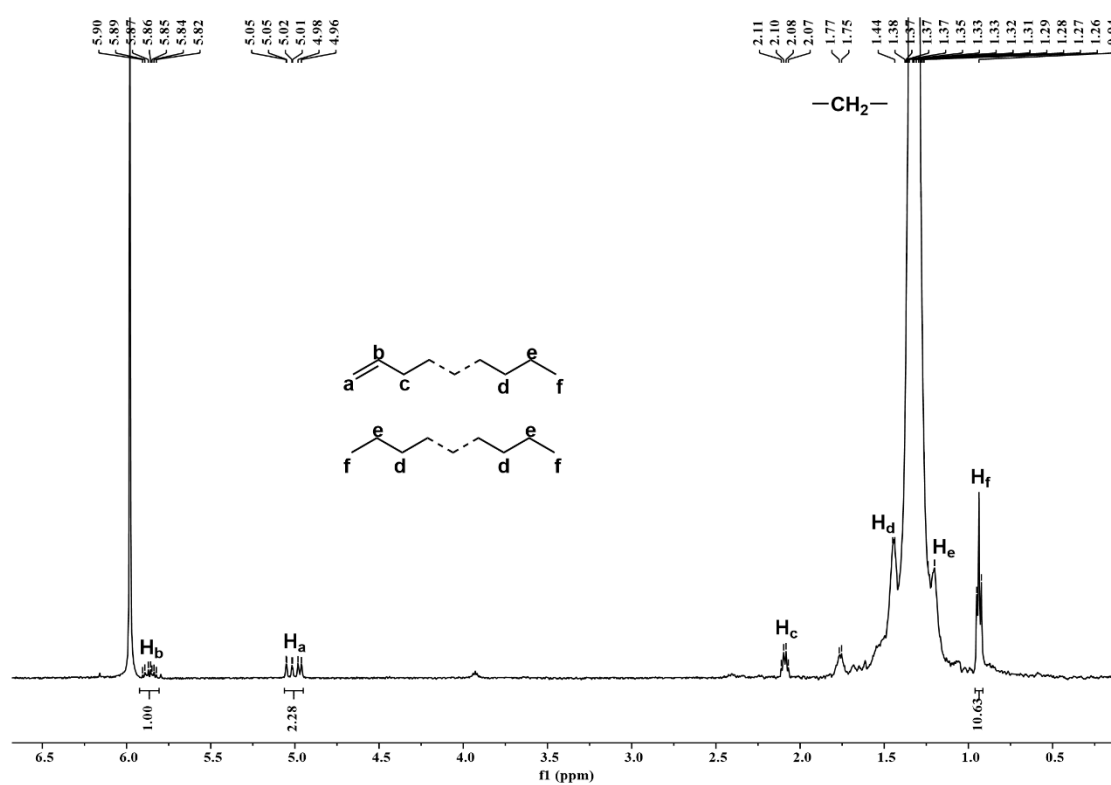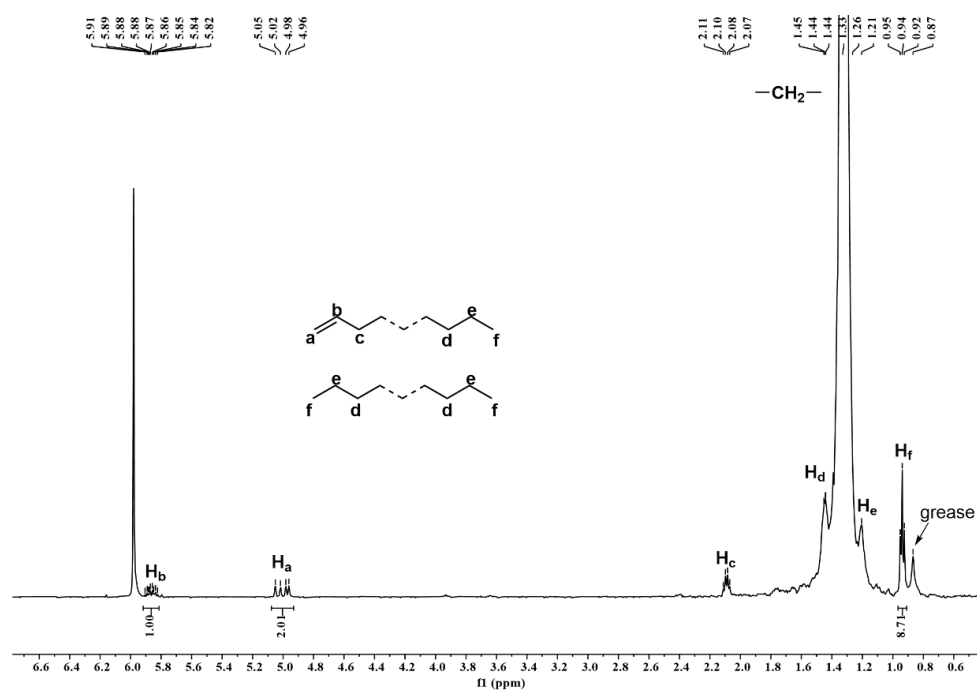

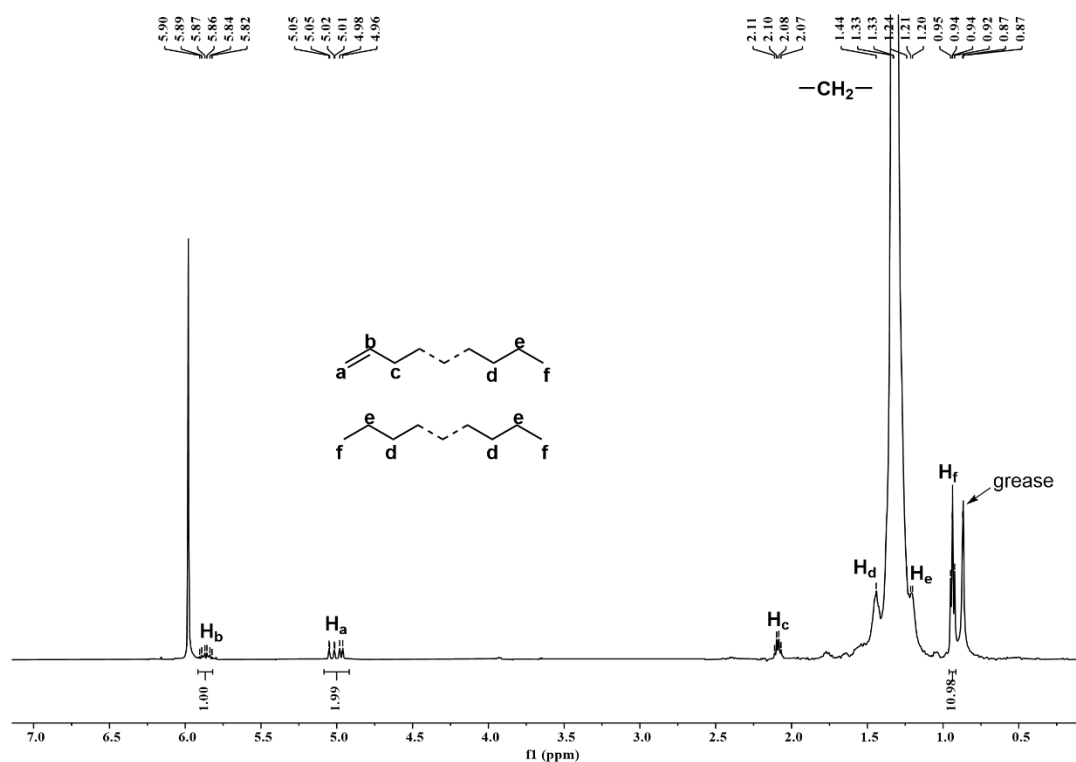**Figure S13.** ^{1}H NMR spectrum of the polyethylene produced using **Fe4**/MAO operating at 80 °C (entry 5, Table 3); recorded at 100 °C in 1,1,2,2-tetrachloroethane-d_2. The weak signal at *ca.* 0.87–0.88 ppm is attributed to the protons belonging to the methyl group in grease [1].

3. Method used to determine the ratio of different end groups in the polymers

On the basis of previous work undertaken using iron ethylene polymerization catalysis [2–4], it has been demonstrated that there can be two different types of end-group in their highly linear polyethylenes, one based on a vinyl group and the other a saturated n-propyl group. As a result, two different polymer chains can be produced, one chain contains a vinyl and a saturated *n*-propyl chain end (chain A, the amount is set as *a*), while the other has both saturated *n*-propyl end-groups (chain B, the amount is set as *b*).
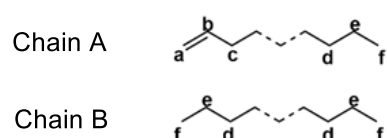
By using the corresponding signals in the ^{1}H NMR spectrum, the integral for the vinyl protons and *n*-propyl protons can then be measured. With regard to the spectra shown in Figures S5-S8 and S9-S13 above, the integral of the vinyl proton H_b can be set as *x*, and the integral of the methyl protons H_f in the n-propyl group can be set as *y*. Then from the equation $a / (3a + 6b) = x / y$, the molar ratio can be expressed as:

$$a / b = 6 / ((y / x) - 3)$$

Tables S1 and S2 show the molar ratios for *a* to *b* in the PE's generated using **Fe4**/MMAO and **Fe4**/MAO at various temperatures, respectively.

Table S1. Determining the molar ratios of *a* (chain A, unsaturated) to *b* (chain B, fully saturated) for the PE's produced using **Fe4**/MMAO at various temperatures.

Run temperature	^{1}H NMR spectrum	Ratio of x / y	Molar ratio, a / b
80 °C (entry 5, Table 2)	Figure 9	1/18.82	0.379
70 °C (entry 4, Table 2)	Figure S5	1/15.02	0.500
60 °C (entry 3, Table 2)	Figure S6	1/6.03	1.980
50 °C (entry 2, Table 2)	Figure S7	1/18.22	0.394
40 °C (entry 1, Table 2)	Figure S8	1/58.73	0.108

Table S2. Determining the molar ratios of *a* (chain A, unsaturated) to *b* (chain B, fully saturated) for the PE's produced using **Fe4**/MAO at various temperatures.

| Run temperature	^{1}H NMR spectrum	Ratio of x / y	Molar ratio, a / b
80 °C (entry 5, Table 3)	Figure S13	1/10.98	0.752
70 °C (entry 4, Table 3)	Figure S12	1/8.71	1.050
60 °C (entry 3, Table 3)	Figure S11	1/10.63	0.786
50 °C (entry 2, Table 3)	Figure S10	1/15.94	0.464
40 °C (entry 1, Table 3)	Figure S9	1/26.66	0.254

4. X-ray crystallographic studies

Table S3. Crystal data and structure refinement for **Fe2** and **Fe3**.

	Fe2·CH₂Cl₂	**Fe3**
CCDC number	2325145	2325146
Empirical formula	$C_{41}H_{47}Cl_4FeN_3$	$C_{44}H_{53}Cl_2FeN_3$
Formula weight	779.46	750.64
Temperature/K	170(2)	169.99(10)
Crystal system	monoclinic	monoclinic
Space group	Ia	P2₁/n
a/Å	12.1167(3)	12.4769(3)
b/Å	19.7628(4)	17.4319(3)
c/Å	16.8845(4)	18.3814(3)
α/°	90	90
β/°	108.717(2)	103.969(2)
γ/°	90	90
Volume/Å³	3829.34(16)	3879.65(14)
Z	4	4
ϱ_{calc}g/cm³	1.352	1.285
μ/mm⁻¹	5.974	4.638
F(000)	1632.0	1592.0
Crystal size/mm³	0.28 × 0.24 × 0.1	0.3 × 0.25 × 0.15
Radiation	CuKα (λ = 1.54184)	CuKα (λ = 1.54184)
2Θ range for data collection/°	7.11 to 154.13	7.09 to 154.68
Index ranges	-15 ≤ h ≤ 15, -24 ≤ k ≤ 9, -17 ≤ l ≤ 21	-14 ≤ h ≤ 15, -19 ≤ k ≤ 21, -23 ≤ l ≤ 18
Reflections collected	13519	32687
Independent reflections	6053 [R_{int} = 0.0305, R_{sigma} = 0.0332]	7922 [R_{int} = 0.1178, R_{sigma} = 0.0730]
Data/restraints/parameters	6053/8/446	7922/259/541
Goodness-of-fit on F²	1.046	0.887
Final R indexes [I>=2σ (I)]	R_1 = 0.0758, wR_2 = 0.1977	R_1 = 0.0672, wR_2 = 0.1997
Final R indexes [all data]	R_1 = 0.0779, wR_2 = 0.2010	R_1 = 0.0825, wR_2 = 0.2219
Largest diff. peak/hole / e Å⁻³	0.67/-0.71	1.66/-0.56

5. FT-IR spectra of Fe1–Fe5
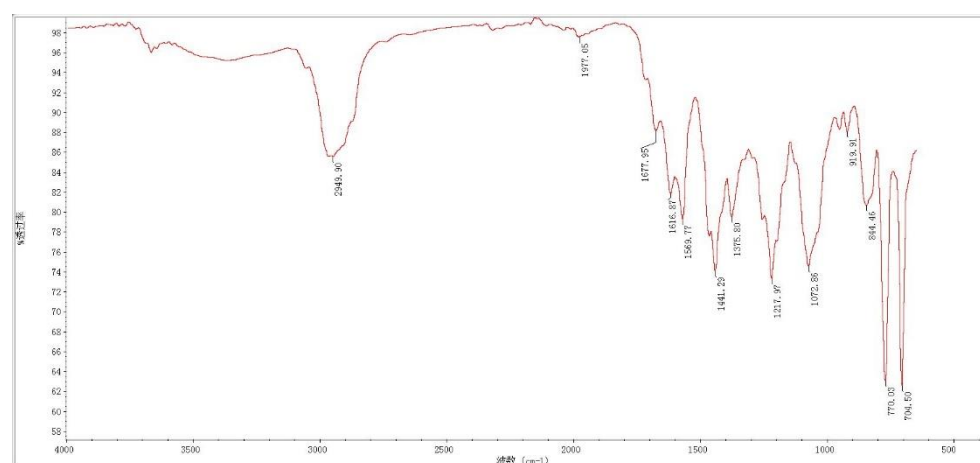
Figure S14. FT-IR spectrum of **Fe1**.

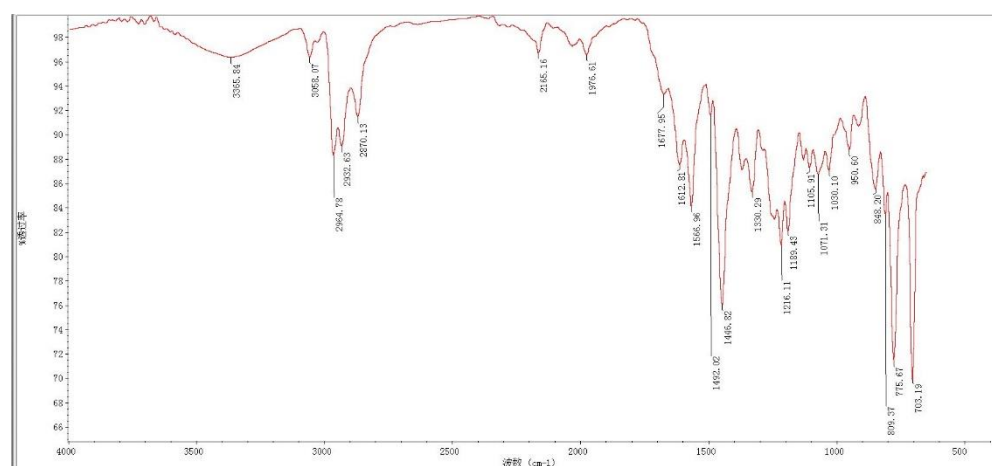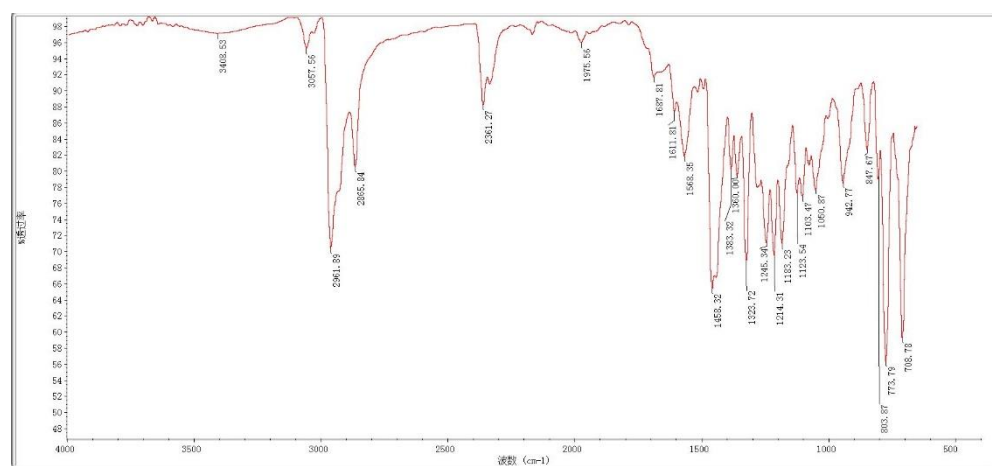**Figure S15.** FT-IR spectrum of **Fe2**.
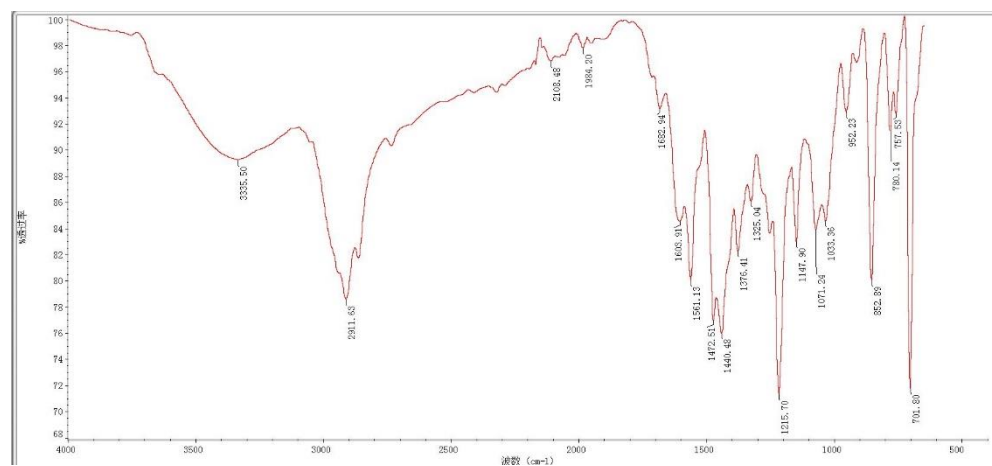

Figure S16. FT-IR spectrum of **Fe3**.

Figure S17. FT-IR spectrum of **Fe4**.
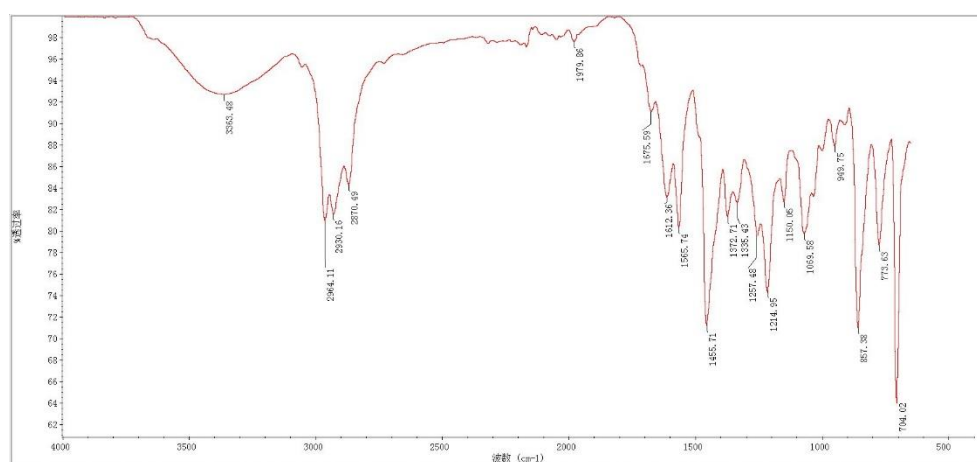
Figure S18. FT-IR spectrum of **Fe5**.

6. Mass spectra of Fe1–Fe5
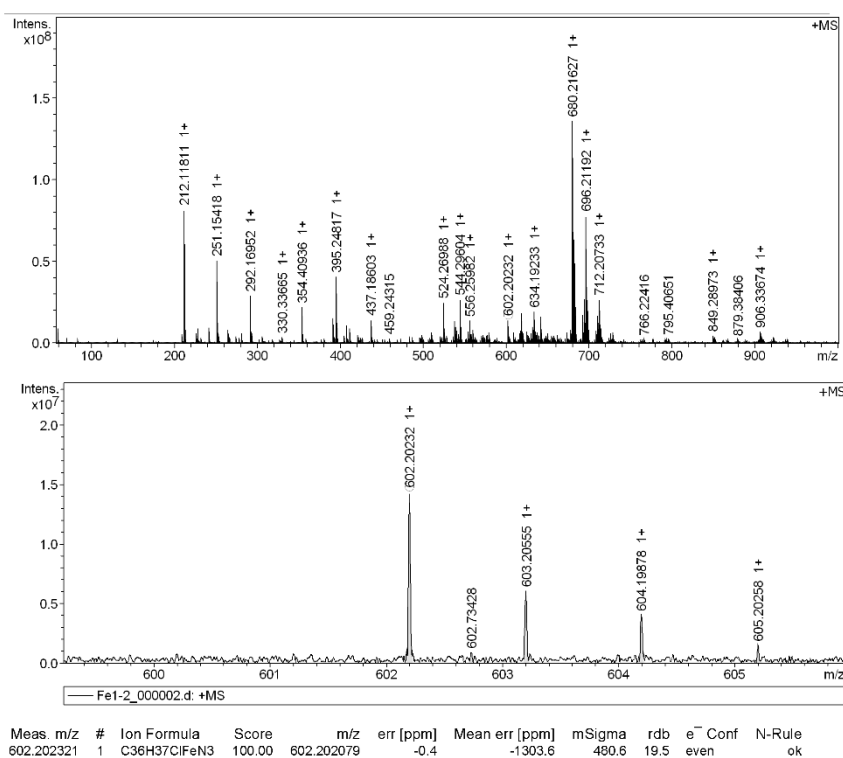
Figure S19. ESI-MS spectrum of **Fe1**.

Meas. m/z	#	Ion Formula	Score	m/z	err [ppm]	Mean err [ppm]	mSigma	rdb	e⁻ Conf	N-Rule
658.264960	1	C40H45ClFeN3	100.00	658.264692	-0.4	0.2	41.6	19.5	even	ok
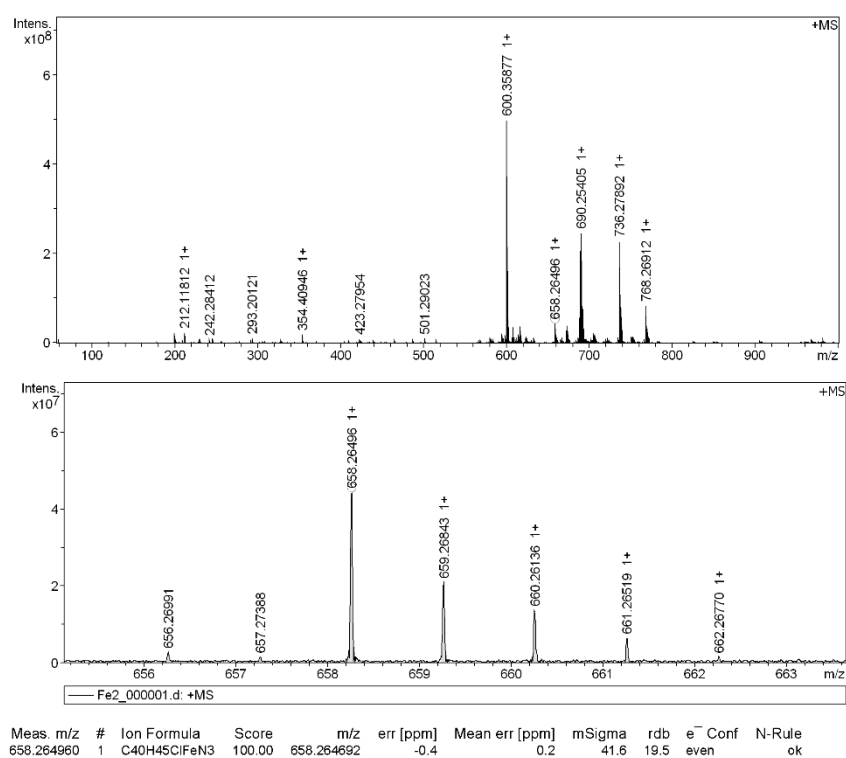
Figure S20. ESI-MS spectrum of **Fe2**.

Meas. m/z	#	Ion Formula	Score	m/z	err [ppm]	Mean err [ppm]	mSigma	rdb	e⁻ Conf	N-Rule
714.327625	1	C44H53ClFeN3	100.00	714.327307	-0.4	0.1	47.8	19.5	even	ok
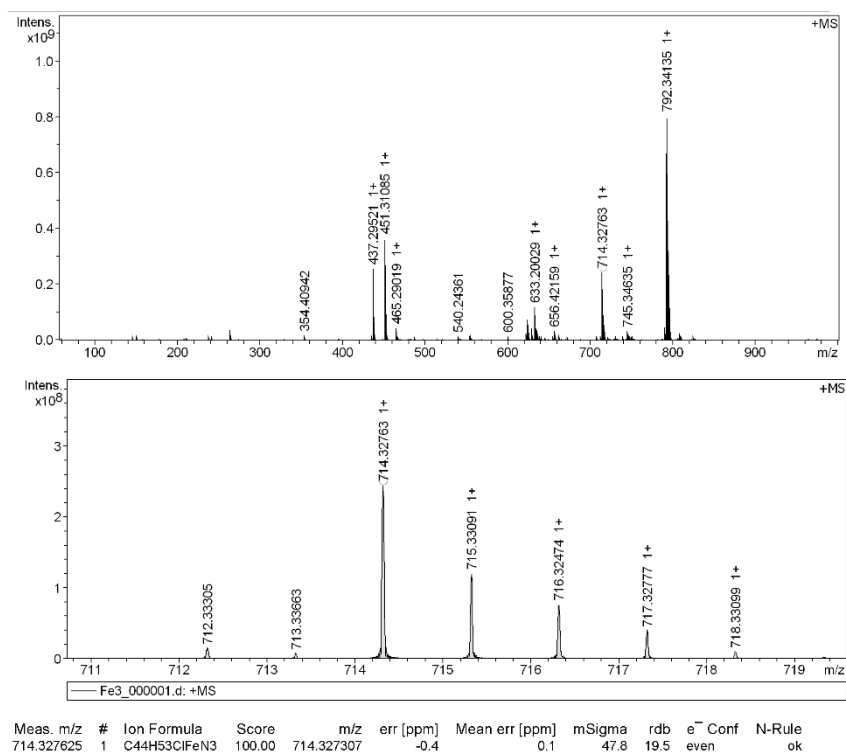
Figure S21. ESI-MS spectrum of **Fe3**.

Meas. m/z	#	Ion Formula	Score	m/z	err [ppm]	Mean err [ppm]	mSigma	rdb	e⁻ Conf	N-Rule
630.233698	1	C38H41ClFeN3	100.00	630.233385	-0.5	0.4	44.6	19.5	even	ok

Figure S22. ESI-MS spectrum of **Fe4**.

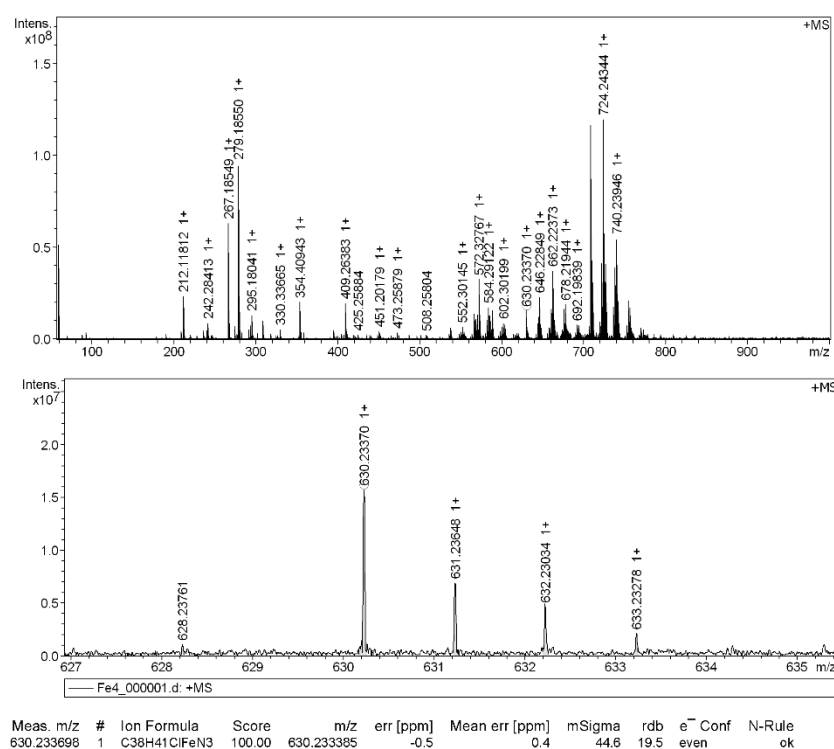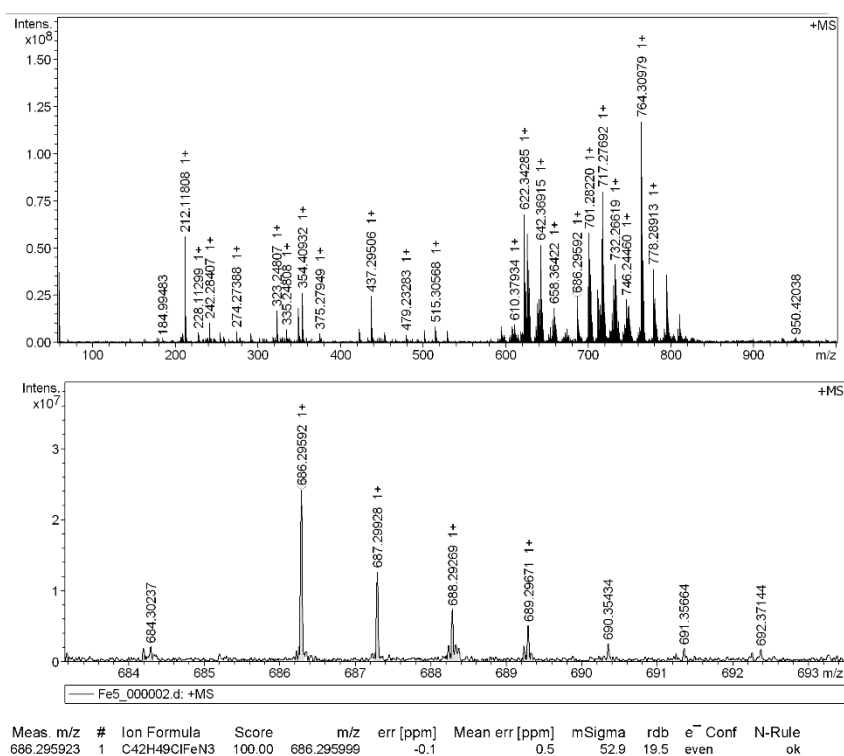| Meas. m/z	#	Ion Formula	Score	m/z	err [ppm]	Mean err [ppm]	mSigma	rdb	e⁻ Conf	N-Rule
686.295923	1	C42H49ClFeN3	100.00	686.295999	-0.1	0.5	52.9	19.5	even	ok

Figure S23. ESI-MS spectrum of **Fe5**.

References

1. Fulmer, G.R.; Miller, A.J.M.; Sherden, N.H.; Gottlieb, H.E.; Nudelman, A.; Stoltz, B.M.; Bercaw, J.E.; Goldberg, K.I. NMR Chemical Shifts of Trace Impurities: Common Laboratory Solvents, Organics, and Gases in Deuterated Solvents Relevant to the Organometallic Chemist. *Organometallics* **2010**, *29*, 2176–2179.
2. Zhang, Q.; Zuo, Z.; Ma, Y.; Liang, T.; Yang, X.; Sun, W.-H. Fluorinated 2,6-bis(arylimino)pyridyl iron complexes targeting bimodal dispersive polyethylenes: Probing chain termination pathways via a combined experimental and DFT study. *Dalton Trans.* **2022**, *51*, 8290–8302.
3. Wang, Z.; Solan, G.A.; Ma, Y.; Liu, Q.; Liang, T.; Sun, W.-H. Fusing Carbocycles of Inequivalent Ring Size to a Bis(imino)pyridine-Iron Ethylene Polymerization Catalyst: Distinctive Effects on Activity, PE Molecular Weight, and Dispersity. *Research* **2019**, *2019*, 9426063.
4. Wang, Y.; Wang, Z.; Zhang, Q.; Zou, S.; Ma, Y.; Solan, G.A.; Zhang, W.; Sun, W.-H. Exploring Long Range para-Phenyl Effects in Unsymmetrically Fused bis(imino)pyridine-Cobalt Ethylene Polymerization Catalysts. *Catalysts* **2023**, *13*, 1387.